Technical University of Denmark

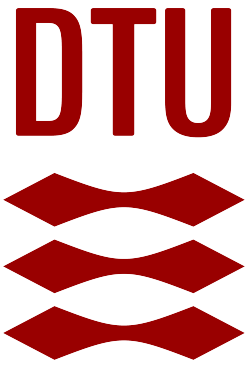

BSc Project

Passive building temperature regulation using VO_2 as a metal-insulator transition material

Monday 16 May 2022

Dania Tareq Pharaon s194774

Supervised by: Jean-Claude Grivel

1 Abstract

VO_2 nanoparticles were developed and studied for their thermochromic properties. A literature review was provided to give an overview of what has been done over the past decades. It was concluded that doping with tungsten was the most optimal, since it provided the largest effect on the transition temperature with each atomic percent added. Five different samples with concentrations 0,1,2,3,4 % at.W doped VO_2 particles were synthesized using a simple hydrothermal technique. The synthesized powders were characterized and compared using X-ray diffraction, scanning electron microscope, X-ray photoelectron spectroscopy, differential scanning calorimetry and UV-Vis spectroscopy. Finally, a simple setup using VO_2 coated bricks was prepared to demonstrate the potential of the prepared samples.

Contents

2 Introduction

Buildings consume around 40% of the total energy consumption in the EU and around 60% goes to space heating [18]. This loss is mostly originating from fabric heat loss; loss through building construction components in the building envelope. Fabric loss was found to amount to around 81% of the total heat energy loss in buildings [16]. Furthermore, with the increase in the CO_2 emissions and electricity prices, new methods for saving energy are necessary to fix this issue. One way to help alleviate this problem is by incorporating thermochromic materials in buildings to help keep them cool in the summer and warm in the winter. Thermochromic materials are materials that undergo an optical change when a temperature change is applied to it. VO_2 has recently been researched more often for its thermochromic properties as it shows a great potential; it can change phases and store thermal energy. However, the main problem is the transition temperature of 68°C. That means the electrical and optical temperatures change at that temperature. For use in residential buildings a lower temperature is needed, and that can be achieved with doping with different elements. It has been found that high valence cation ions such as W^{+6} , Mo^{+6}, Nb^{+5} and Ta^{+5} have been found to decrease the transition temperature when doped with VO_2 [7]. Lower valence cations have an opposite effect.

VO_2 exists in many phases: VO_2(A)(tetragonal), VO_2(B)(monoclinic), VO_2(M)(monoclinic-rutile), VO_2(R)(tetragonal rutile), as well as VO_2(D) and VO_2(B) etc [14]. VO_2(B) is being used as a cathode material in Lithium batteries. Furthermore, VO_2(A) is being researched for use in batteries too, since it has a larger capacity when compared to VO_2(B) and V_2O_5 [4]. It is however not very useful in energy saving applications since it has a transition temperature of about 162°C.

However, VO_2(M) is one of the most interesting one for building energy saving purposes, as it shows a fully reversible first-order metal-to-insulator transition (MIT) with the phase transition temperature (T_c) at about 68°C, accompanied by a crystallographic transition between the low temperature monoclinic phase (M) and a high temperature tetragonal phase (R). The monoclinic phase is semi conductive and is relatively IR transparent. The tetragonal phase on the other hand, is metallic and is reflective of IR light. Furthermore, the tetragonal phase filters out the infrared radiation but maintains the visible light transmission and therefore doesn't affect the lighting inside a building. For that reason VO_2 has been used for smart window applications which is shown in figure 1.

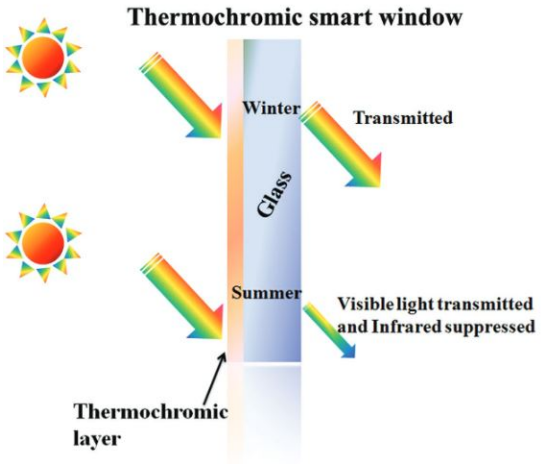

Figure 1: Illustration of a thermochromic smart window [14]

The vanadium dioxide used will be in powder form, because powders, unlike thin films, are found to be more suitable for standing the stresses induced by phase change [17].

The aforementioned phase change was found in [6] and later explained in [3]. In the metallic phase, a wide π and a narrow π^* anti-bond are formed between the V^{+4} and the O^{-2} orbitals a $d_{||}$ nonbond is also formed between adjacent V^{+4} orbitals. The phase is metallic because the $\pi*$ and the $d_{||}$ bands partially overlap and the Fermi level lies where they overlap. This however changes in the insulating phase when the temperature decreases. A 0.7 eV band gap forms between the $\pi*$ and the $d_{||}$ bonds, which leads to the insulating phase. Figure 2 shows the atomic and band structures of the two phases. It can be seen that one of the major changes in the atomic structure is the V-V distancing in the two different phases. It is a constant length of 2.85Å in the tetragonal phase and it changes to an alternating pattern of lengths 2.60Å and 3.19Å.

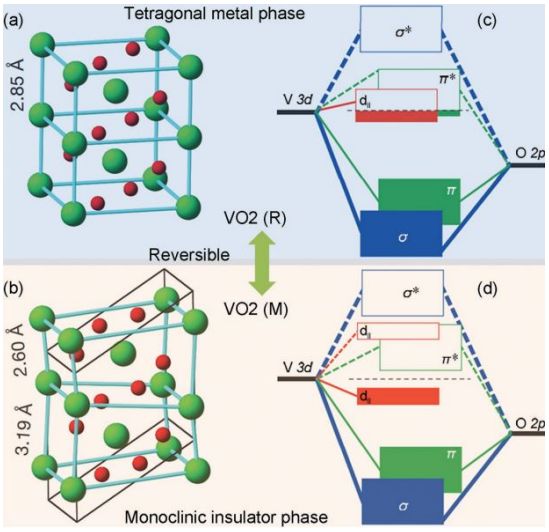

Figure 2: Side by side comparison of the M and R phase [14]

2.1 Literature Review

It was found in [17] that the doping amount of Tungsten was proportional to the transition temperature of VO_2. A doping percentage of around 2 at.% was needed to lower the transition temperature to temperatures close to room temperature. J. Shi et al found that the the amount of the doped W content in VO2 particles could be easily controlled by the concentration of the W precursor as the amount of Tungsten in the feed was linearly proportional to the Tungsten in the W-doped VO_2 particles [20]. The same linear relationship was found by [25], however only until dopant concentrations of around 3-4%. Furthermore, doping with more than 6% was found to have a negative impact on the transition temperature of the doped VO_2.The minimum transition temperature of 40°C was obtained when doping with 4% W. It was concluded that the reason for that was that adding dopants beyond a certain extent weakened the lattice and impeded the growth of VO_2, since it is easier for a pure material to grow in a crystal than for a doped material to grow.

In [13], Li et al. explored the possibility of co-doping with a high-valence element like Tungsten and a low-doping element like Magnesium. It has previously been found that Magnesium increases the transition temperature by 22°C per at.% for Mg amounts less than 1%. This explains why doping W-doped VO2 with Mg increases the transition temperature, and that is due to the charge compensation effect; substituting the low-valence Mg^{+2} dopants for high-valence W^{+6} in the V^{+4} lattice. However, it was found that another effect was also realized, and that is the increased band gap and luminance transmittance which is useful in window applications. It was concluded that the W+Mg combination wasn't very effective. Guo et al.[7] deduced that co-doping with either of the combinations: W/Zr and W/Mg, showed an improvement in both the transition temperature and the transmittance. Jiazhen et al found that co-doping with Mo and W doesn't result in the superposition of the individual influence of the separate elements, in fact the effect was larger than if they were doped individually [9].

A low cost carbothermal approach (using graphite as a reducing agent) for synthesizing VO_2 and W-doped VO_2 samples was developed by [26] where the decrease of the transition temperature was found to be ~24°C, which is one of the highest values found.

It was found that the reason for the lowering of the transition temperature when doping with W is that the W breaks up the $V^{+4} - V^{+4}$ bonding and causes the transfer of two 3d electrons to the nearest V ions for charge compensation, forming two new bonds: $V^{+3} - W^{+6}$ and $V^{+3} - V^{+4}$ The semiconducting phase is destabilized when the $V^{+4} - V^{+4}$ bond is broken which causes the transition temperature to decrease [21]. Chen et al.[24] doped VO_2 with Mo in a facile inexpensive way by using molybdenum acid as a dopant. Increased doping lowered the transition temperature but reduced the dopant efficiency. A transition temperature of 54.8°C was obtained when doping with 2%at of Mo^{+6}. It was confirmed that the decrease in transition temperature was due to the fact that the larger Mo^{+6} substituted the smaller V^{+4} atoms and decreased the band gap, therefore enabling electron transmission between the bands. However, it was also deduced that the increase in doping imposed strains and defects in the lattice which impeded the aforementioned electronic transmission.

Batista et al. [2] compared the three elements W, Mo and Nb and their influence on the

transition temperature and the IR modulation efficiency. Niobium causes a significant amount of defects in the crystal lattice which clearly degrade the optical properties while reducing the semiconductor-metal transition to room temperature. Whereas Tungsten showed the greatest increase in the transition temperature of VO2. As observed, the semiconductor metal phase transition exhibits a characteristic thermal hysteresis which is due to latent heat evolved and absorbed during the first-order structural transition. The shifting of the hysteresis loops to lower temperatures as a consequence of the increasing contents of substitutional W in the VO2 solid solution is very clearly seen.

Table 1: Review of papers with doping using different elements

Technique	Doping Elements	Doping Percentage	Source
Thermolysis	W	20	[17]
Hydrolysis	W	27	[20]
Sol-Gel method	W+Mo	Effect was non-linear	[9]
Hydrothermal	W	7 (Effect is non-linear after 2%)	[25]
Carbothermal	W	24.14	[26]
Solid-state reaction	W	28.1	[19]
Thermolysis	W	16.5	[12]
Dual-target reactive magnetron sputtering	Mo	12	[10]
DC & pulsed-DC reactive magnetron sputtering	W/Mo/Nb	7/3/2	[2]

Despite all the advantages of incorporating VO_2 in building materials, several disadvantages exist and therefore the innovation still has more potential for improvement. One of the main issues with dealing with VO_2 is its chemical and physical stability. The VO_2 is not the most stable vanadium oxide and therefore it always tends to change to another more stable vanadium oxide. Upon contact with moisture VO_2 can undergo changes that will affect its thermochromic abilities, as is seen in section 4.2.

Following this review section, the experimental section will go over the techniques and methods used in this report. It was decided that is would be best to focus on doping with Tungsten with a hydrothermal technique. A direct synthesis of VO_2(M) was preferred due to the extremely high annealing temperatures (higher than 400°C) are needed to producing VO_2(M) with a two-step reaction from a different phase such as VO_2(B) or VO_2(A) [14].

3 Experimental techniques

3.1 Synthesis

The VO_2 and doped VO_2 powders were synthesized by a water-based hydrothermal strategy using V_2O_5 (Sigma-Aldrich, USA) as the source of vanadium and citric acid (H2C2O4 · 2H2O, Alfa Aesar GmbH & Co KG, Germany) as a reducing agent. Tungsten was used as doping agent from ammonium tungstate ($(NH_4)_{10}H_2(W_2O_7)_6$, Sigma-Aldrich, USA). All of the chemical reagents used in the experiments were analytical grade without further purification. In a typical procedure, 0.688g of V_2O_5 and 2.38g citric acid solid powder were directly added to 55 ml deionized water at room temperature. The suspension was continuously stirred for around 24 hours until a clear dark blue solution was formed. The solution was transferred into a Teflon-lined autoclave with a stainless steel shell followed by hydrothermal treatment under auto-generated pressure at 200°C for 24 hours. For W-doped samples, 1,2,3 and 4 at.% tungsten samples were prepared. 0.02, 0.041, 0.062 and 0.083g was added to the same solution from before. Again, the suspension was continuously stirred for around 24 hours until a clear dark blue solution was formed. The solution was transferred into a Teflon-lined autoclave with a stainless steel shell followed by hydrothermal treatment as described before. After the hydrothermal treatment, the autoclave was cooled naturally to room temperature. The resulting precipitates were collected by filtering, washed with deionized water, then dried in air at 50°C for another 24 hours. In section 4.2, glass films needed to be coated with the VO_2 particles. This was done by preparing a poly vinyl alcohol (PVA) mixture and then mixing the VO_2 in it. In order to prepare the PVA sample, 50ml of water was heated to 50°C and stirred for a few minutes and then 2.5g of PVA was added gradually. As for the developed bricks discussed in section 4.3, they were coated with a mix of the VO_2 sample and poly vinyl acetate. The mixture was placed on the bricks and then heated in the furnace at 250°C for 3-4 hours.

3.2 Characterization

3.2.1 X-Ray Diffraction

X-ray diffraction (XRD) analysis was conducted out on a Rikagu 600 diffractometer at a scanning rate of 2° per minute with 2θ ranging from 15 to 60 degrees, using graphite monochromated Cu Kα1 radiation ($\lambda = 0.154056$ nm) at 40 KV accelerating voltage and 15 mA current. XRD is a method used to investigate the crystalline phases and orientation of a material. XRD is carried out firstly by generating X-Rays and then hitting the material with them. The reflected rays are then measured and analyzed to determine the structure of the material, as well as other information such as the existing phases and the size of the internal stresses [11]. X-Rays are electromagnetic radiation that have wavelengths that are on the scale of inter-atomic distances, whereas visible light has longer wavelengths. X-Rays generated when a heated filament releases high speed electrons which then bombard a metal target often made of Copper or Aluminum etc. The reflected rays can interfere constructively or destructively depending on the phase difference of the rays. A difference that is an even multiple of π is constructive and therefore, adds

up. Otherwise, the interference would be destructive and would cancel out. The intensity of the peaks in an XRD graph are caused by the superposition of the constructive and destructive contributions. Bragg diffraction occurs in the case of constructive interference and the following equation would then apply:

$$n\lambda = 2dsin(\theta) \tag{1}$$

d is the distance between the different atomic layers, the angle θ is the angle of incidence of the X-Rays and λ is the wavelength of the incident radiation.

Figure 3 shows the setup in a XRD experiment. The source is usually fixed, however both the sample and the detector would move gradually to cover the range of angles specified in the beginning of the experiment with the given step size.

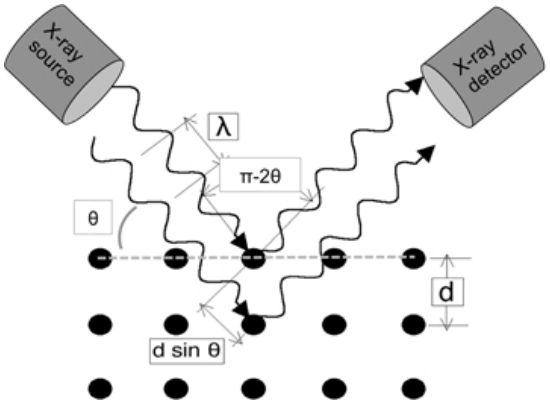

Figure 3: Illustration of Bragg's Law [11]

The final result is a graph of intensity against 2θ. From Bragg's law, it can be seen how the angle and d are related. Lower angle peaks are caused by larger inter atomic distances.

3.2.2 X-Ray Photoelectron Spectroscopy

The XPS (X-ray Photoelectron Spectroscopy) works on the photoelectric effect discovered by Einstein. It is a nondestructive characterization technique that works on the outermost 10 nm of a material [5]. When electrons absorb enough energy after being hit by x-ray radiation, they are emitted from the sample. The kinetic energy of the emitted electrons is measured in the electron energy analyzer and counted in the electron detector. XPS is therefore a method used to identify the elements existing on the sample's surface as well as their chemical states. It is also used to give information on the environment the element is in. The detector detects electrons differently as they would be traveling different paths, and therefore it would be able to distinguish between the different electrons and therefore produce different peaks. Each element in nature has a distinct electronic arrangement (different amount of electrons distributed between the s,p,d and f orbitals), and the farther away from the nucleus an atom is the smaller the binding energy. This explains why p orbitals are always to the right of d orbitals (assuming a descending scale). When the X-rays hit the surface of the sample with a known photon energy, the emitted electron KE is measured in the analyzer. The X-rays used in this report are Al kα with an energy of

1486.7 eV. According to the photoelectric effect equation, the binding energy of the emitted electron would then be the only unknown left:

$$E_{kinetic} = E_{photon\ (h\nu)} - E_{binding} - \varphi$$

The XPS instrument used in this report was the Thermo Scientific™ ESCALAB™ 250Xi X-ray Photoelectron Spectrometer (XPS) Microprobe.

3.2.3 Scanning Electron Microscope

The microscope used in this project is the Scanning Electron Microscope. It is very suitable for analyzing powder samples that are capable of remaining stable in vacuum. Another advantage of using SEM is the relatively short time needed for preparing the samples and analyzing it. Using a Scanning Electron Microscope (SEM), the surface topography and composition can be non-destructively found, i.e without causing volume loss in the sample. That is done when a focused beam of electrons scans the surface of the specimen to be investigated. The aforementioned focused beam can be produced when primary electrons are generated and passed through an anode and later condensing lenses that control the beam diameter and current. When the beam hits the surface of the sample it then decelerates and produces a variety of different signals, including the secondary, backscattered and the diffracted backscattered electrons. The secondary electrons (produced by inelastic scattering) are utilized for showing the morphology and the topography of the sample's surface since the electrons are emitted from the first few nanometers of the sample.

Whereas, the backscattered electrons (produced by elastic scattering) are utilized for imaging different phases and elements in the material. SEM was used in combination with Energy-Dispersive X-Ray Spectroscopy (EDS) to analyze the emitted x-ray's energy spectrum and create a element composition map that illustrates the elements contained in the sample as energy peaks. The SEM used in this report is the Hitachi TM3000 Tabletop Scanning Electron Microscope.

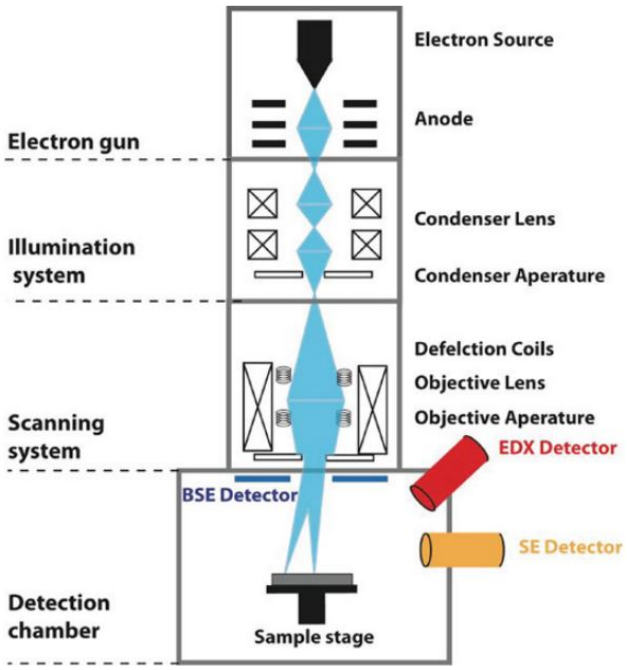

Figure 4: Schematic of SEM [8]

3.2.4 Other Equipment used

Phase transition temperature and its hysteresis property were measured by differential scanning calorimetry (DSC 200 F3 Maia Differential Scanning Calorimeter, NETZSCH Premier Technologies) in a heating or cooling rate at 5°C/min with a liquid nitrogen cooling system. DSC is a thermal analysis techniques used to measure the temperature transition in a material. The UV-Vis spectrum ranging from 190 to 1100 nm was measured using the VWR UV-3100PC spectrophotometer.

4 Results & Discussions

4.1 Structural Characterization

Crystal structures of the developed samples was characterized by XRD. All the samples spectra are shown figure 5. The peaks around 28°, 37° , 41° ,56° , 58° and 65° are typical VO_2(M) peaks corresponding to the (011), ($\bar{2}$11), (020) , (220) , (022) and (002). However the peak at around 47° can't be found in a VO_2(M) sample, but it is could be a VO_2(A) peak. The reason a pure VO_2(M) sample was not achieved could be either because the molar ratio of the reactants was not optimal or that the synthesis temperature wasn't high enough [1]. In Alie et al, it is argued that the ratio of oxalic acid to vanadium pentoxide determines the phase of the resulting VO_2. A lower amount of oxalic acid produces VO_2 predominantly in the A phase, whereas a higher amount of oxalic acid produces VO_2 in the M phase. Another experiment was done by the same group to test out the difference the heating temperature has on the resulting product. It was shown that temperatures around 300°C were necessary to have a pure M phase without impurities.

A slight shifting to the left in the (011) phase peak is observed with increasing of the Tungsten concentrations. In addition to that, the peak widens with higher concentrations of dopant, which can be attributed to the increase of dopant defects which causes severe lattice distortions. The difference between the size of Tungsten and Vanadium is found to be the reason for this peak shifting. The radius of V^+4 is ∼72pm and the radius of W^+6 is ∼74pm citeWradius ,[22]. When Tungsten is added to the VO_2 lattice the d spacing was then found to increase [20].

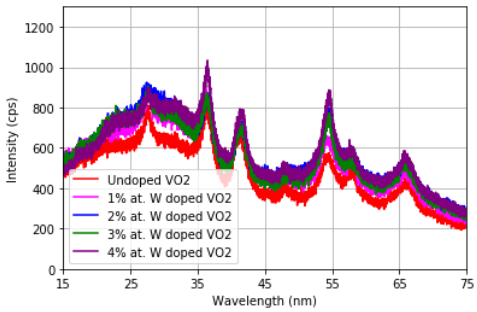

(a) XRD spectrum for all samples

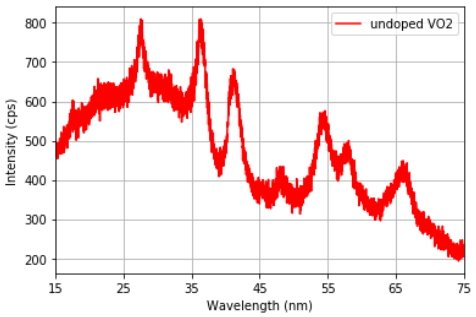

(b) Undoped VO_2

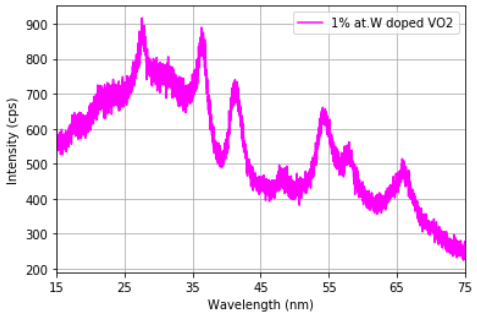

(c) 1% at.W doped VO_2

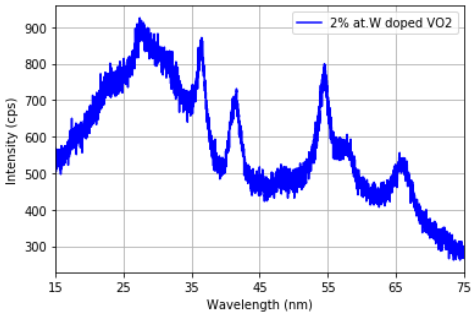

(d) 2% at.W doped VO_2

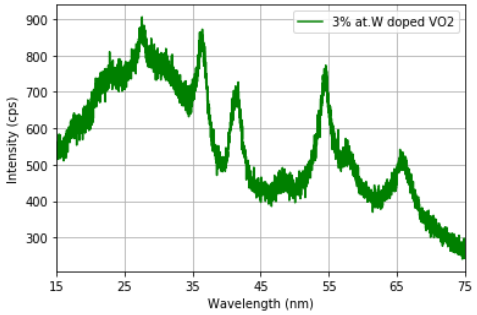

(e) 3% at.W doped VO_2

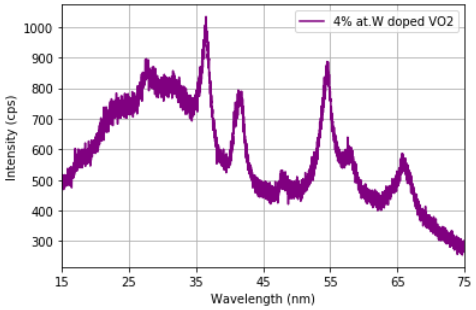

(f) 4% at.W doped VO_2

Figure 5: XRD spectra

Figures 6 to 9 compare the XPS spectra of the doped and undoped VO_2 samples. As it can be seen in figure 7, the $V_{2p_{3/2}}$ peak can be found around 516.6 eV in both samples. In figure 8, the O_{1s} peak can be found at around 530 eV in both samples. A C_{1s} can be found in both samples at around 285 eV due to unavoidable surface contamination.

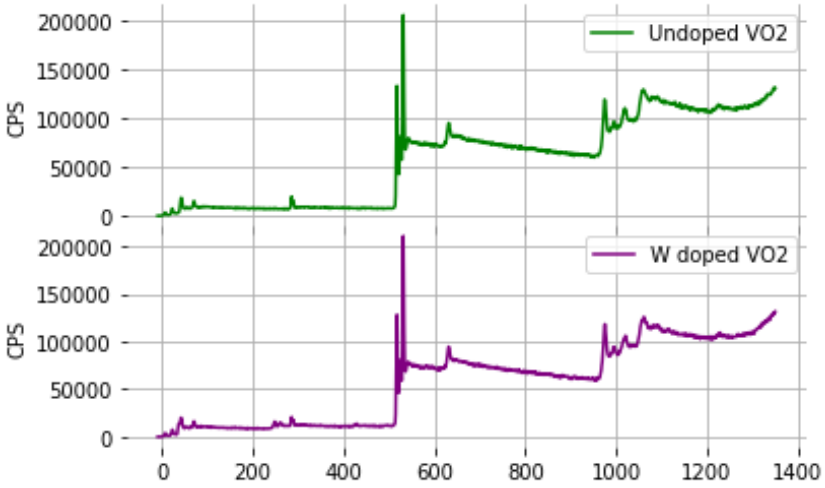

Figure 6: Full XPS spectra

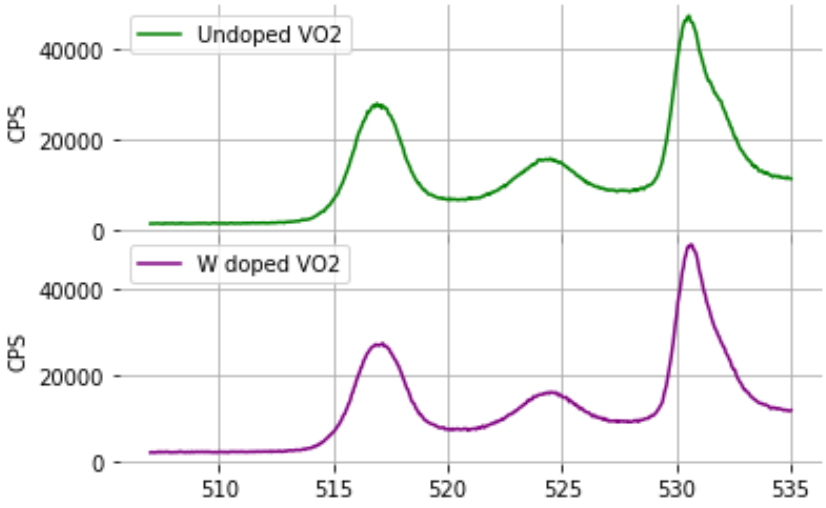

Figure 7: 515-535 eV spectra XPS

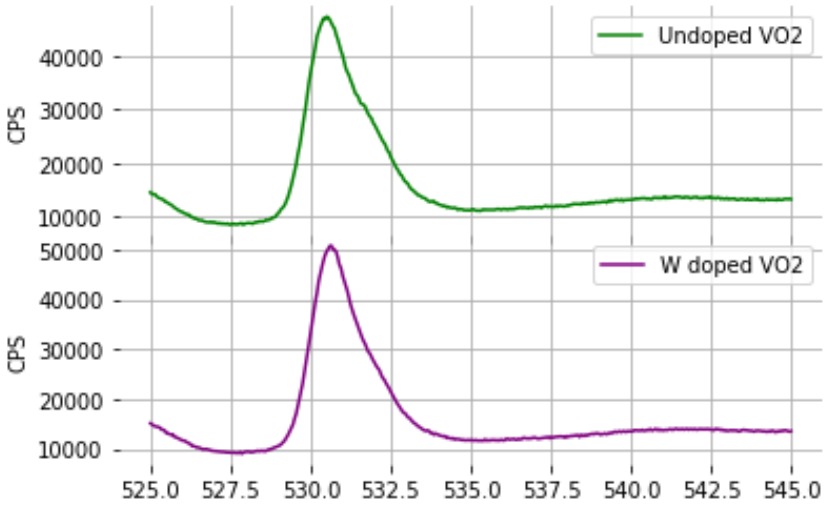

Figure 8: 525-545 eV spectra XPS

The major difference can be seen in figure 9 where the peaks at 35.5 eV and 37.8 eV can be attributed to the $W_{4f7/2}$ and $W_{4f5/2}$ respectively, this indicates the successful synthesis of W-doped VO_2 particles. The handbook shows very similar values for the aforementioned peaks [15].

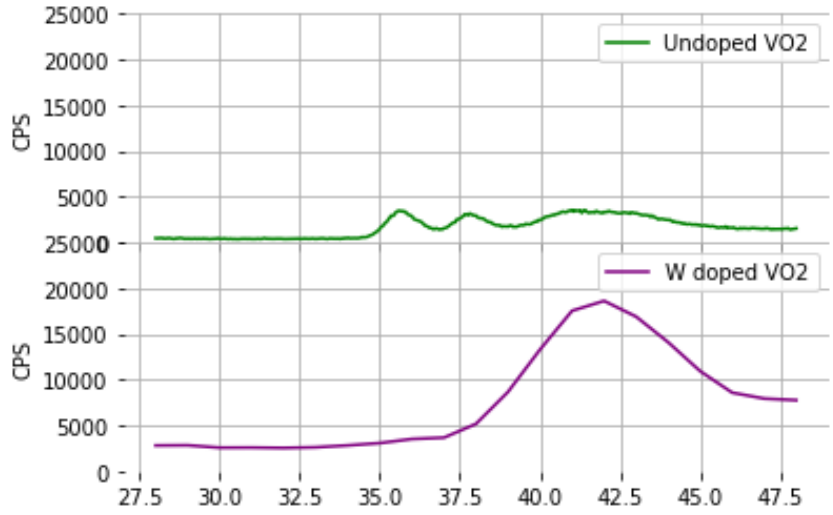

Figure 9: 28-48 eV spectra XPS

Figure 10 show the SEM images for undoped VO_2 and 2% at. W doped VO_2. As it can be seen the particle size distribution is very broad. It was found by Xiao et al. [23] that the overall size of the particles decreases with the increase of dopant concentrations. The reason for that can be attributed to the fact that the increase in the W content hinders the growth of crystalline grain.

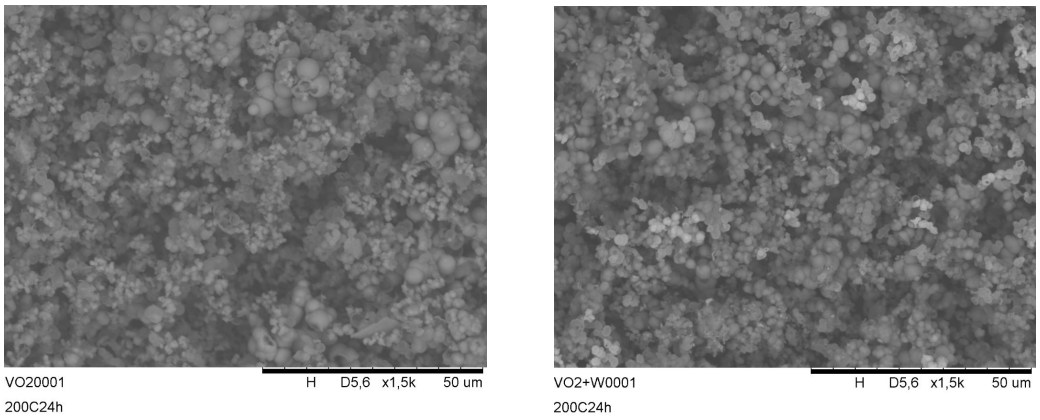

(a) SEM image of undoped VO_2 (b) SEM image of doped VO_2

Figure 10: SEM images

EDS images for the two samples are shown in the section 8. EDS data showed a 2% atomic percentage of tungsten in the 2% W doped VO_2 sample which goes in accordance with the linear relationship discussed in section 2.1.

Differential scanning calorimetry was carried out with the following temperature changes: ~25°C-> -20°C -> 120°C > -20°C. A baseline measurement was taken as a control and then two other measurements were taken. One was of the undoped VO_2 and the other was of the 2 at.% W doped VO_2.

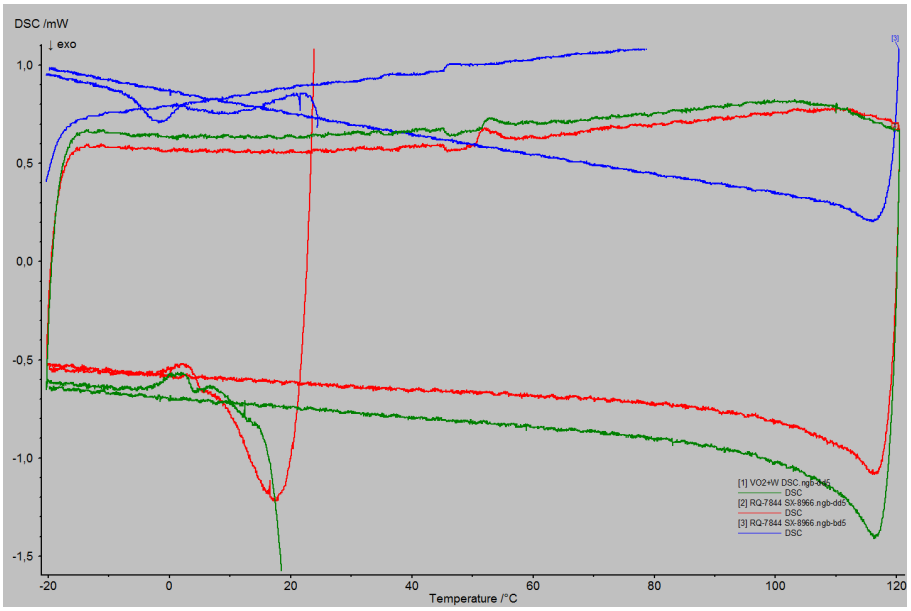

Figure 11: DSC of doped (green) and undoped (red) VO_2 and baseline (blue) measurements

The reason no clear peaks were found was not really found. One possibility could be due to the not entirely monoclinic phase as was seen in the XRD plots. More experiments would be needed to be certain of the aforementioned point.

4.2 Optical analysis

The optical properties of the developed VO_2 samples were studied using the UV-Vis spectrometer. It can be seen in figure 12 that the optical transmittance is decreasing with an increase in the doping concentration of Tungsten. The maximum transmittance is around 40% in the infrared region for the undoped VO_2 sample. Furthermore, very similar results can also be seen in the literature [2]. This can be explained by the phase switching that is occurring with an increase in the W amounts in the sample.

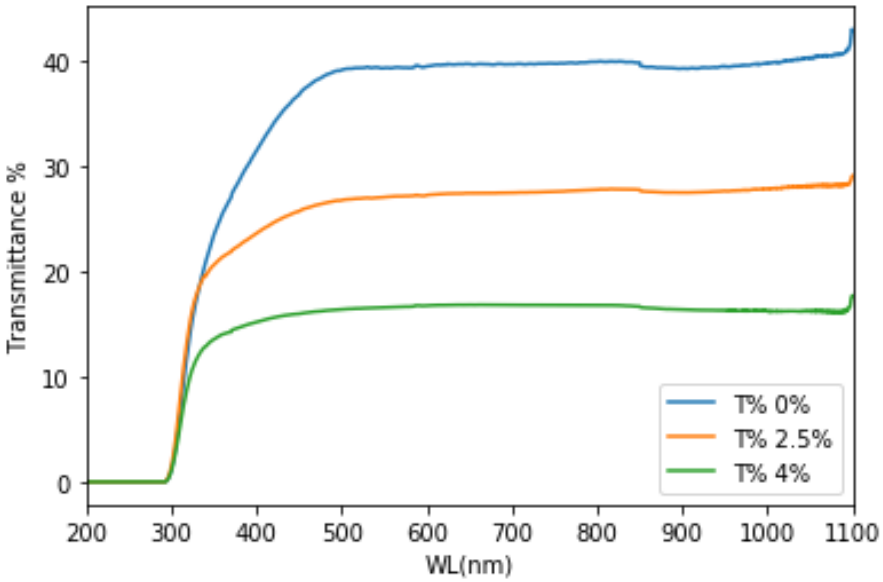

Figure 12: Difference in transmittance % with different doping quantities

In order to get the best possible results, three glass films were coated and analyzed in the spectrometer for each of the three samples. Afterwards, the average was taken due to the slight variability in the results.

Afterwards, the coated glass films were connected to a heating element inside the UV-Vis spectrometer in order to observe the phase change when going from a temperature below to a temperature above the transition temperature. However, since the poly vinyl alcohol samples were synthesized with water, the phase switching was not observed and the transmittance kept constant throughout a range of temperatures of 22°C to 80°C. The reason for that is believed to be because the VO_2(M) can be oxidized to vanadium oxides or their hydroxides in the presence of moisture [3].

4.3 Bricks Setup

This section aims to show the potential of the developed VO_2 samples at storing energy for longer periods of time. Two primitive brick setups were developed. One was a control and the other was coated with 2% at.W doped VO_2. The two setups went through the same heating program which consisted of 15 minutes of heating at 130°C. Afterwards, the furnace was turned off and the brick setups were left to cool naturally. Figure 13 shows the two brick setups.

(a) Top view (b) Side view

Figure 13: Pictures of bricks setup

Figure 14 shows the resulting temperature vs. time curves for the two setups. As it can be seen the coated setup took longer time to reach room temperature and that is deemed to be due to the developed sample's thermal storage abilities.

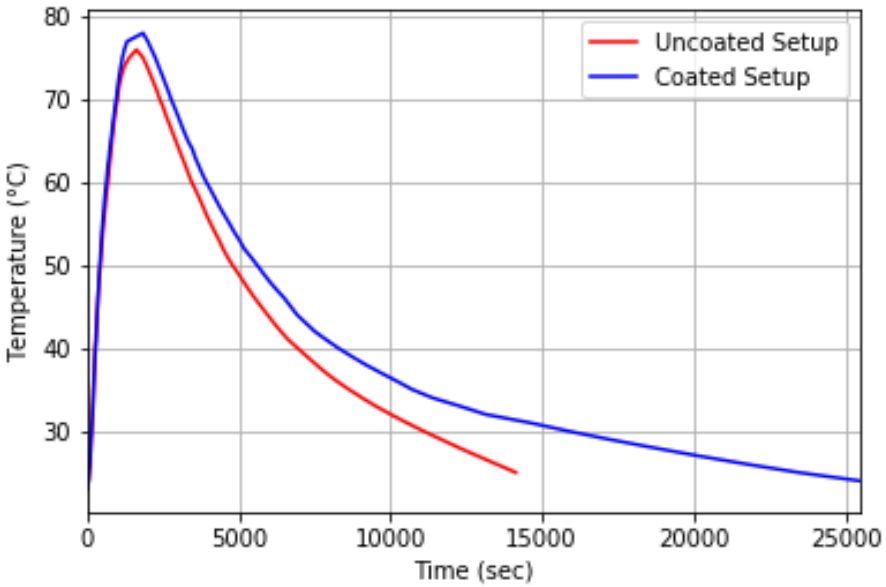

Figure 14: Comparison of two brick setups

5 Conclusion

Doped and undoped VO_2 samples were synthesized using a simple hydrothermal method and characterized by different methods such as XRD, XPS etc. It was found in the literature that Tungsten was the most effective dopant at bringing down the transition temperature. The drawback to adding too much dopant is increased dopant defects and strains as well as decreased optical transmittance. The W dopant had almost no influence on the crystal structure of VO2 particles. Only a slight shift of the (110) peak toward small reflection angle was observed with increasing W-doping fraction. It was found that VO_2 required certain conditions to fully transform into the M phase. More experimentation could have provided more certainty in this regard. A simple setup was developed to demonstrate the potential of the material developed. It showed thermal storage abilities, however the exact temperature where the phase change occurred could not be pinpointed.

References

[1] David Alie et al.
"Direct synthesis of thermochromic VO2 through hydrothermal reaction".
In: Journal of Solid State Chemistry 212 (2014), pp. 237–241.
DOI: https://doi.org/10.1016/j.jssc.2013.10.023.

[2] Carlos Batista, Ricardo M Ribeiro, and Vasco Teixeira.
"Synthesis and characterization of VO2-based thermochromic thin films for energy-efficient windows".
In: Nanoscale Research Letters 6.301 (2011).
DOI: https://doi.org/10.1186/1556-276X-6-301.

[3] Yuanyuan Cui et al.
"Thermochromic VO2 for Energy-Efficient Smart Windows".
In: Joule 2 (2018), pp. 1707–1746.
DOI: https://doi.org/10.1016/j.joule.2018.06.018.

[4] L. Dai et al.
"VO2 (A) nanostructures with controllable feature sizes and giant aspect ratios: one-step hydrothermal synthesis and lithium-ion battery performance".
In: RSC Advances 2 (2012), pp. 5265–5270.
DOI: 10.1039/C2RA20587D.

[5] Imaging David Mogk and Montana State University Chemical Analysis Laboratory.
X-Ray Photoelectron Spectroscopy (XPS; aka Electron Spectroscopy for Chemical Analysis, ESCA).
URL: https://serc.carleton.edu/msu_nanotech/methods/xps.html (visited on 05/16/2022).

[6] JOHN B. GOODENOUGH.
"The Two Components of the Crystallographic Transition in VO2".
In: JOURNAL OF SOLID STATE CHEMISTRY 3 (1971), pp. 490–500.
DOI: https://doi.org/10.1016/0022-4596(71)90091-0.

[7] H. Guo et al.
"Influence of dopant valence on the thermochromic properties of VO2 nanoparticles".
In: Ceramics International 47.15 (2021), pp. 21873–21881.
DOI: https://doi.org/10.1016/j.ceramint.2021.04.205.

[8] X. Jiang, T. Higuchi, and H. Jinnai.
"Scanning Electron Microscopy".
In: Molecular SoftInterface Science (2019), pp. 141–146.

[9] Yan Jiazhen et al.
"Effect of Mo-W Co-doping on semiconductor-metal phase transition temperature of vanadium dioxide film".
In: Thin Solid Films 516.23 (2008), pp. 8554–8558.

DOI: https://doi.org/10.1016/j.tsf.2008.05.021.

[10] P. Jin and S. Tanemura.
"V1xMoxO2 thermochromic films deposited by reactive magnetron sputtering".
In: Thin Solid Films 281-282 (1996), pp. 239–242.
DOI: https://doi.org/10.1016/0040-6090(96)08641-5.

[11] MA JoVE Science Education Database.JoVE Cambridge.
X-ray Diffraction.
2022.
URL: https://www.jove.com/v/10446/x-ray-diffraction (visited on 04/17/2022).

[12] F.Y. Kong et al.
"Synthesis and thermal stability of W-doped VO2 nanocrystals".
In: Materials Research Bulletin 46.11 (2011), pp. 2100–2104.
DOI: https://doi.org/10.1016/j.materresbull.2011.06.030.

[13] Donglai Li et al.
"Influence of the charge compensation effect on the metal–insulator transition of Mg-W co-doped VO2".
In: Applied Surface Science 579.151990 (2022).
DOI: https://doi.org/10.1016/j.apsusc.2021.151990.

[14] Ming Li et al.
"Hydrothermal Synthesis of VO2 Polymorphs: Advantages, Challenges and Prospects for the Application of Energy Efficient Smart Windows".
In: Small 13.36 (2017), p. 1701147.
DOI: https://doi.org/10.1002/smll.201701147.

[15] Jolm F. Moulder et al.
Handbook of X-ray Photoelectron Spectroscopy.
1993.

[16] Mohammad K. Najjar et al.
"A framework to estimate heat energy loss in building operation".
In: Journal of Cleaner Production 235 (2019), pp. 789–800.
DOI: https://doi.org/10.1016/j.jclepro.2019.07.026.

[17] Zifei Peng, Wei Jiang, and Heng Liu.
"Synthesis and Electrical Properties of Tungsten-Doped Vanadium Dioxide Nanopowders by Thermolysis".
In: The Journal of Physical Chemistry C 111.3 (2007), pp. 1119–1122.
DOI: 10.1021/jp066342u.

[18] Marie Rousselot and Frédéric Pinto Da Rocha (Enerdata).
ENERGY EFFICIENCY TRENDS IN BUILDINGS IN THE EU.
2021.

URL: https://www.odyssee-mure.eu/publications/policy-brief/buildings-energy-efficiency-trends.html (visited on 05/02/2022).

[19] Nan Shen et al.
"Lowered phase transition temperature and excellent solar heat shielding properties of well-crystallized VO2 by W doping".
In: Physical Chemistry Chemical Physics 18.40 (2016), pp. 28010–28017.
DOI: 10.1039/c6cp05143j.

[20] Jianqiu Shi et al.
"Preparation and thermochromic property of tungsten-doped vanadium dioxide particles".
In: Solar Energy Materials and Solar Cells 91.19 (2007), pp. 1856–1862.
DOI: https://doi.org/10.1016/j.solmat.2007.06.016.

[21] C. Tang et al.
"Local atomic and electronic arrangements in W VtO2".
In: PHYSICAL REVIEW B 31.2 (1985), pp. 1000–1011.
DOI: 10.1103/PhysRevB.31.1000.

[22] Vanadium: radii of atoms and ions.
URL: https://www.webelements.com/vanadium/atom_sizes.html (visited on 05/16/2022).

[23] Xiudi Xiao et al.
"Thermochromic VO2 for Energy-Efficient Smart Windows".
In: Materials Research Bulletin 51 (2014), pp. 6–12.
DOI: https://doi.org/10.1016/j.materresbull.2013.11.051.

[24] Y.Chen, W. D. Liang, and H. Xu.
"Effect of Mo on phase transition temperature of VO2 nanopowders".
In: Materials Research Innovations 14.2 (2010), pp. 173–176.
DOI: 10.1179/143307510X12639910071791.

[25] Yifu Zhang et al.
"Preparation of W- and Mo-doped VO2(M) by ethanol reduction of peroxovanadium complexes and their phase transition and optical switching properties".
In: Journal of Alloys and Compounds 544 (2012), pp. 30–36.
DOI: https://doi.org/10.1016/j.jallcom.2012.07.093.

[26] Juntao Zou et al.
"A simple method to prepare V1-xWxO2 (x = 0, 0.01, 0.02, 0.03, 0.04, and 0.05) controllable phase transition temperature powder".
In: Journal of Alloys and Compounds 708 (2017), pp. 706–712.
DOI: https://doi.org/10.1016/j.jallcom.2017.03.081.

6 List of figures

7 List of tables

8 Appendix

8.1 EDS figures

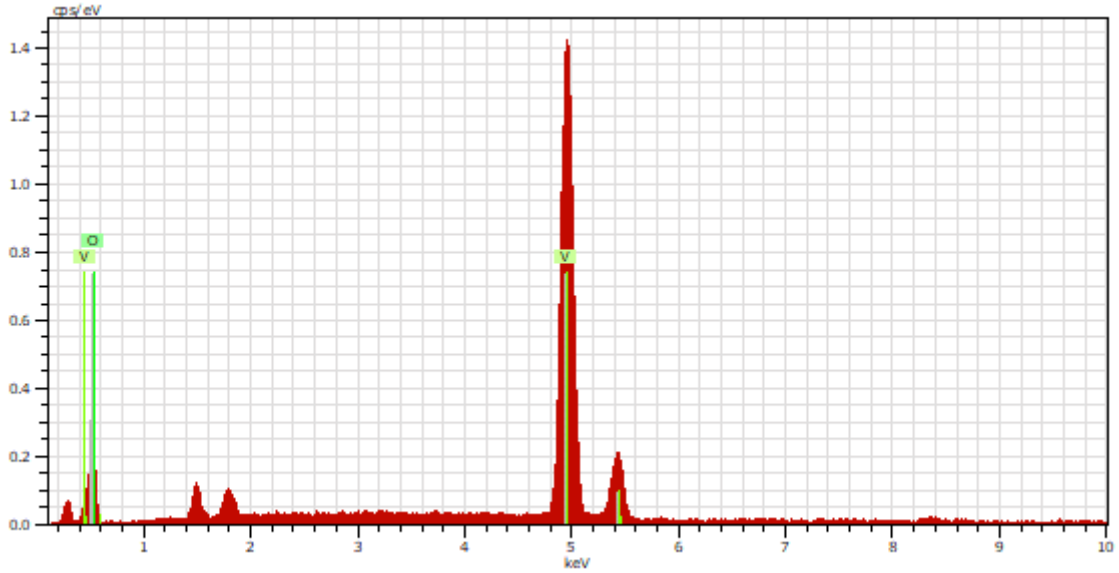

Figure 15: EDS spectrum of VO_2

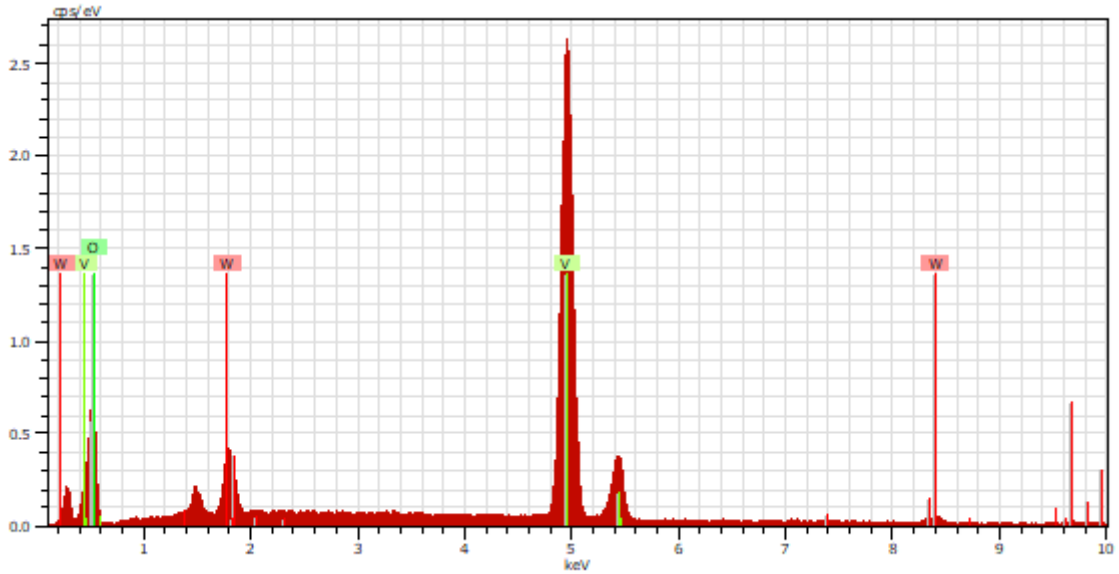

Figure 16: EDS spectrum of W doped VO_2

8.2 Thermal Analysis

Figure 17 shows 6 selected times where there was a noticeable change in the peaks. The first graph shows the characteristic H_2O. The rest of the graphs show a sharp peak at around 2200 cm^-1 which is a characteristic CO_2 peak.

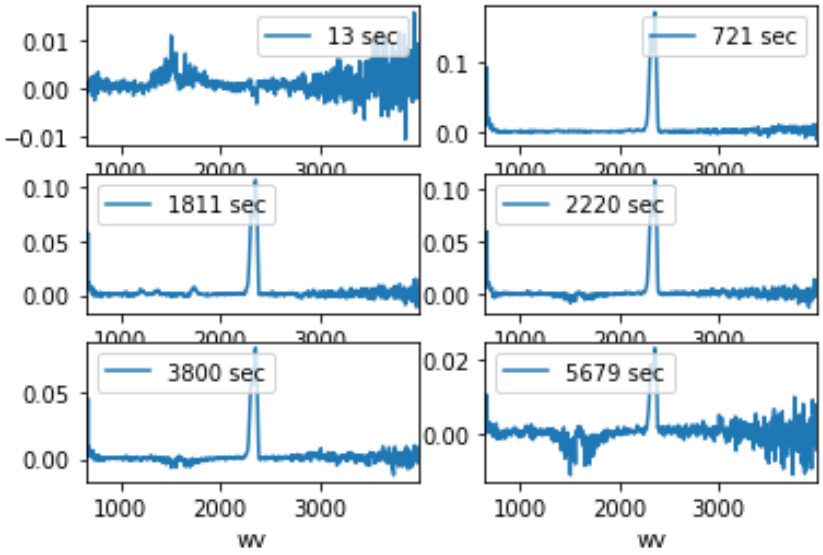

Figure 17: FTIR spectra for 6 selected times